PAPER Special Section on Multi-dimensional Mobile Information Networks

Using Large-Scale FDTD Method to Obtain Precise Numerical Estimation of Indoor Wireless Local Area Network Office Environment

Louis-Ray HARRIS[†a)], *Nonmember*, **Takashi HIKAGE**[†], *and* **Toshio NOJIMA**[†], *Members*

SUMMARY The Finite-Difference Time-Domain (FDTD) technique is presented in this paper as an estimation method for radio propagation prediction in large and complex wireless local area network (WLAN) environments. Its validity is shown by comparing measurements and Ray-trace method with FDTD data. The 2 GHz (802.11b/g) and 5 GHz (802.11a) frequency bands are used in both the calculations and experiments. The electric field (E-field) strength distribution has been illustrated in the form of histograms and cumulative ratio graphs. By using the FDTD method to vary the number of human bodies in the environment, the effects on E-field distribution due to human body absorption are also observed for 5 GHz WLAN design.

key words: *finite-difference-time-domain (FDTD) method, wireless local area network (WLAN), indoor propagation, histogram, human absorption*

1. Introduction

The number of devices that communicate using wireless networks has been rapidly increasing in recent years and the devices' transmission frequencies continue to increase. It is also common for large data files to be sent over these networks. In a well-designed wireless local area network (WLAN) environment, there should be good signal coverage throughout the entire area so that portable devices do not experience any signal interruptions. In the case of indoor WLANs, signal reflection, refraction and absorption are important factors that must be considered since a good WLAN radio propagation service area estimation requires signal coverage to remain above a predefined minimum value. When there are many complex objects, it also becomes a multi-reflective environment. When designing indoor WLANs, it is also necessary to consider the optimum number of access points (APs) to be used and the best positions in which they should be placed for optimum data throughput. This is very important because the overall cost of a WLAN design will increase unnecessarily if there are too many APs [1].

Generally, estimation methods like Moment of Methods (MoM) [2], [3] and Ray-Tracing [4]–[9] are used for estimating propagation distribution in large WLAN environments that consist of multiple objects. In complex multi-reflective environments with many objects, the Finite Difference Time Domain (FDTD) method [10], [11] can also be used to consider electrical properties of various objects.

The aim of this paper is to highlight the applicability of the FDTD method when estimating E-field distribution in large-scale WLAN office environments. However, for large-scale modeling, the required amount of memory is very high, requiring the use of a supercomputer. The validity of the FDTD method in large and complex multi-reflective environments is established by comparing data obtained from FDTD calculations with data obtained experimentally and using the Ray-trace method.

Additionally, the absorption effect due to human bodies can be considered. The need for investigations into the shadowing effect by the human body has become more important [12]. We believe that human absorption effects are not negligible so an estimation method allowing this effect to be considered is desired. Up to this point, there has not been extensive research investigating the suitability of the ray-tracing and MoM methods in determining the absorption effect of human bodies. A key advantage of the FDTD method over other estimation methods is that simple modifications allow the inclusion of human phantom models' parameters in order to deduce the human absorption effect. In the context of an indoor WLAN it is useful to be able to estimate the extent to which the performance of the WLAN is impacted under conditions when varying numbers of humans are present.

In Sect. 2, field strength estimation methods that are used are explained. In Sect. 3, the validity of the FDTD method in this type of environment is shown by comparing the calculation results with results obtained using experimental and ray-tracing methods. Section 4 examines the variation in FDTD calculated field strength values in cases when the number of humans in the environment changes. As a result, the applicability of large-scale FDTD analysis in indoor propagation estimation is established.

2. Field Strength Estimation Methods

This section explains the parameters that were used in the models to achieve the various results using the FDTD, Measurement and Ray-tracing methods.

Manuscript received December 26, 2008.
Manuscript revised April 9, 2009.
[†]The authors are with Hokkaido University, Sapporo-shi, 060-0814 Japan.
a) E-mail: louis@emwtinfo.ice.eng.hokudai.ac.jp
DOI: 10.1587/transfun.E92.A.2177

2.1 Office Room Model

The room and the objects that it contained were modeled to-scale. Each of the objects has different electrical parameters [13] which are listed in Table 1. Figures 1 and 2 illustrate 2- and 3-dimensional diagrams of the modeled office room. Its dimensions are 10 m × 3.6 m × 16 m and some of the objects it contains are desks, bookshelves, chairs, metal partitions etc.

Table 1 FDTD, room & signal parameters.

Cell size (cubic)	d = 1cm × 1cm × 1cm
Absorbing Boundary	PML (8 layers)
Problem Space	1134×1509×364 (WxLxH) (including PML and guard cells)
Signal Frequency	2.4 GHz & 5.2 GHz
Access Point	Dipole antenna;(vertical polarization) Input Power 100mW
Materials of Room model [13]	Concrete Walls/Roof: ε= 4.5; tan δ= 0.0111 Plastic: ε= 3.2; tan δ= 0.416 Cushion (Air): ε= 1.0; tan δ= 0 Wooden doors: ε= 3.0; tan δ= 0.005 Glass: ε= 6.5; tan δ= 0.002 Floor/Desks/Bookshelves/ Partitions/Refrigerator: Metal(Perfect electric conductor)

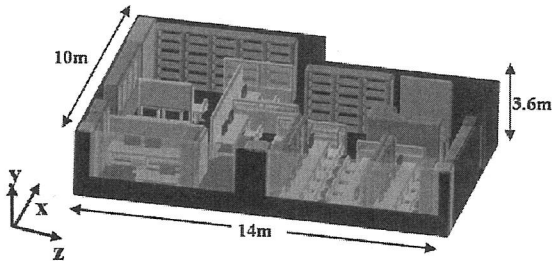

Fig. 1 3-dimensional model of room that has been modeled.

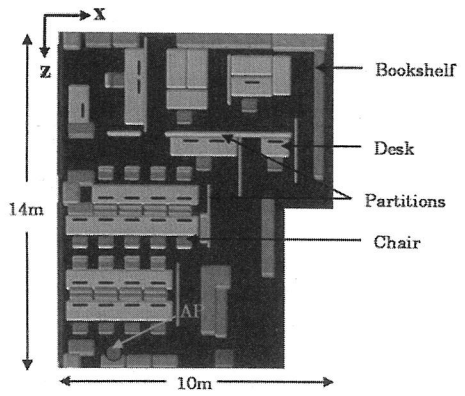

Fig. 2 2-dimensional visualization of room model.

2.1.1 Furniture

There were over 20 desks which were each 0.7 m high. There were 22 chairs which all had plastic and cushion components. There were 3 different types of metal partitions with heights ranging from 1.2–1.8 m and there was also a metal locker that was 1.9 m tall and 2.4 m wide. 28 bookshelves were located around the room and these were mainly made of metal (1 was made of wood). There were also 4 floor-to-ceiling concrete posts that were each 1.3 m wide. Other objects such as computer monitors, a sink and a refrigerator were also present.

2.1.2 Access Point

The two frequency bands used in the simulations were IEEE 802.11b/g (2.4 GHz) and 802.11a (5.2 GHz). The transmitting antenna was a dipole antenna with a signal power of 100 mW. The AP was placed at a height of 2.65 m above the floor at the location shown in Fig. 2. This height was chosen since it corresponds to a location in the actual environment at which test equipment can be setup in the experimental part of the study. The estimation plane in which calculations were done was 1.0 m from the floor because wireless devices tend to be placed at that approximate height whether on a desk or in someone's hand as they stand or walk. The field polarization of the transmitting antennas was vertical and the calculated measurements assumed vertical polarization of |E|.

2.2 FDTD Model

Numerical simulations were carried out using a Hitachi SR11000 Series supercomputer cluster that allowed parallel processing of calculations in different nodes. The peak performance of a node is 121.6 GFLOPS.

The room was divided into 6 nodes each having dimensions $1134 \times 251 \times 364$ cm. Approximately 600 GB of RAM was needed. However, this is well within the capabilities of the computer system used and the CPU runtime was 5 hours 19 minutes per simulation. The total amount of RAM actually used for each node was less than 100 GB but additional memory allows for expansion of the model for calculations of |E| in multi-storey environments.

In the FDTD analysis, a cell size of 1 cm was chosen. This is considered sufficient for obtaining accurate results for both frequencies since it is $0.08\,\lambda$ for 802.11b/g and $0.17\,\lambda$ for 802.11a. The resulting number of cells at which the E-field strength is calculated is about 622 million.

A general rule of thumb concerning the choice of cell size requires that it be smaller than the wavelength of the highest transmitted frequency. A cell size of $0.1\,\lambda$ is considered to be a good approximation but when cell sizes ranging between $0.08\,\lambda$ and $0.17\,\lambda$ are chosen, it is also possible for reasonable results to be obtained [14]. 802.11b/g and 802.11a have wavelengths of λ = 12.5 cm and λ = 5.8 cm

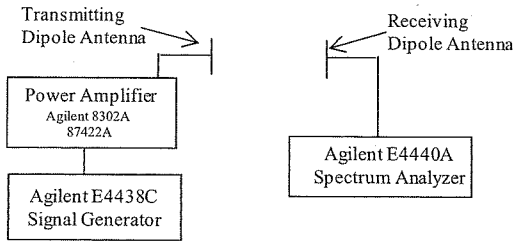

Fig. 3 Block diagram of measurement apparatus.

Table 2 Antenna factor and cable loss for measurement.

Frequency (GHz)	Antenna Factor (dB)	Cable Loss (dB)
2.4	35.7	1.8
5.2	43.5	2.8

respectively. When the above criteria are considered, the chosen value (1 cm) falls within the acceptable range. Using this value, it is determined that the total number of cells in the problem space, each of which is a 1 cm cube, is approximately 622 million.

2.3 Experimental Setup

The AP configuration during the measurements was the same as during the FDTD calculations (with respect to polarization, frequency, transmission power and position).

A block diagram showing the setup of the measuring equipment is shown in Fig. 3. The entire area of the room was divided into squares having a spacing of 50 cm apart and measurements were taken 50 cm apart at the corners of each square at a height of 1.0 m from the floor. Based on this division method, the total number of points to be measured was 540 but due to the physical obstacles such as concrete posts, a metal locker among others, a maximum of only 526 measurements could be taken. The E-field strength was calculated using the equation:

$$\bar{E} - Field\ \ Strength = V_{in} + AF + L_c\ (\mathrm{dB}\mu\,\mathrm{V/m}) \quad (1)$$

where: V_{in} = Spectrum Analyzer input voltage, AF = antenna factor of the dipole antenna, and L_C = cable losses. Table 2 shows the antenna factor and cable loss values.

2.4 Ray-Trace Parameters

Ray-trace data was obtained using an omni-directional receiving antenna. When the simulations were performed, the receiving area from which the data was obtained was 1 cm^2. The transmitting antenna was a dipole antenna with frequencies of 2.4 GHz and 5.2 GHz and a transmission power of 100 mW (the same as the measurement and FDTD parameters). The heights of the AP and the estimation planes are the same as in the FDTD model. Almost all furniture in the room is also similar but the chairs were not present and simple-shaped bookshelves are used in the ray-trace model. The maximum signal reflections of up to 10 times were considered. Ray-trace simulations also took into account signal diffraction throughout the area and these simulations were carried out using proprietary ray-tracing software.

3. Establishing the Validity of Large-Scale FDTD Estimation Method

3.1 Two Dimensional Field Distributions Using FDTD, Ray-Tracing and Measurement Methods

Figures 4 and 5 and Figs. 6 and 7 illustrate in 2-D form the data in the plane 1 m above the floor for FDTD and Measurement data respectively. In total, there were over 1.6 million data points for which the E-field strength was calculated using FDTD. Figures 8 and 9 also provide a similar comparison for data obtained using the Ray-tracing technique as outlined in Sect. 2.4.

Blue areas in Figs. 4, 5, 8 and 9 represent areas with perfect conductors hence the values of |E| were zero. Blue areas in Figs. 6 and 7 represent locations where the receiving antenna could not be set. The distributions illustrate the E-field strength reduction in the estimation plane 1 m from the floor as distance from the AP increases.

From Figs. 4, 5, 8 and 9, it is possible to see the shadowing, reflection and diffraction effects of partitions and other objects on the transmitted signals since the resolution of the distributions is higher than that of the measurement. The Ray-tracing results in Figs. 8 and 9 also show regions where |E| is strongest and how the calculated values vary as distance from the AP increases. A visual comparison of the FDTD and Ray-tracing results indicates that the FDTD results show more of the intermediate values of |E| that fall between the peak value near the AP, and the lowest values far from the AP.

3.2 Comparing FDTD, Measurement Data and Ray-trace Data Using Histograms

In order to obtain a more complete understanding of the distribution of the calculated and measured data for the entire area, it is proposed that histograms be used as they allow the frequency of occurrence of all values in a 2 dimensional matrix to be displayed on a graph. In this way, the relative weighting of different values in an entire estimation plane is obtained and it is then possible to predict whether a network's coverage exceeds a certain threshold level. In E-field histograms, for each value of E-field strength, the frequency of occurrence is shown as a percentage of all the values in the room. This illustration gives a good visualization of dominant signal strength values in the room. This was done and they are shown in Figs. 10 and 11. These figures also include data obtained using the Ray-tracing method.

The histograms' shapes and range of data values are similar and when the calculated FDTD data from the entire plane (over 1.3 million points) are compared with measured data from the entire plane (526 points) and Ray-tracing data (over 1.3 million points), there is a very good correlation between the three sets of data.

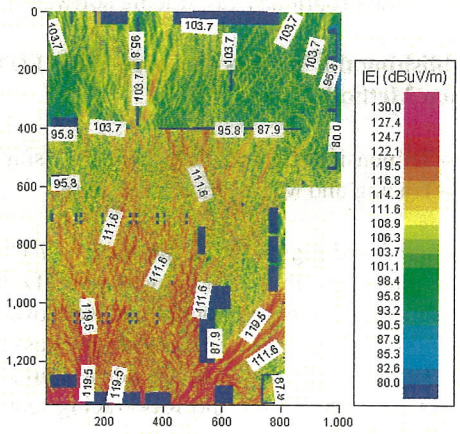

Fig. 4 FDTD data 1.0 m above the floor for 2.4 GHz.

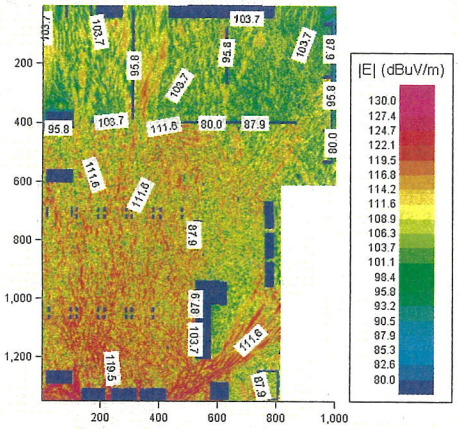

Fig. 5 FDTD data 1.0 m above the floor at 5.2 GHz.

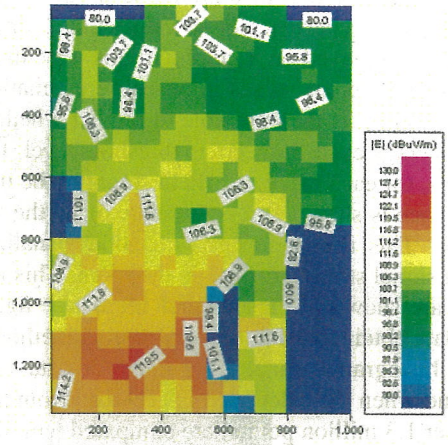

Fig. 6 2.4 GHz Experiment data with adjacent points spaced 50 cm apart.

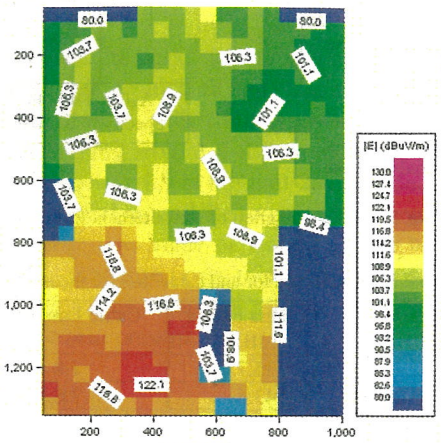

Fig. 7 5.2 GHz Experiment data with adjacent points 50 cm apart.

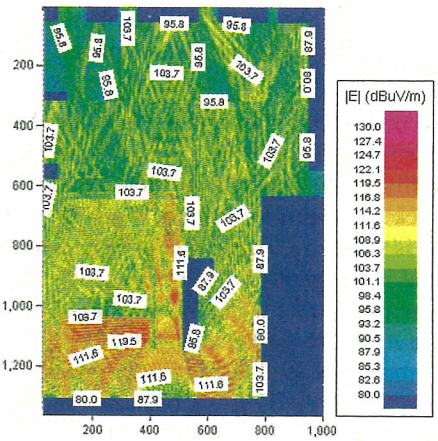

Fig. 8 Ray-tracing data 1.0 m above the floor at 2.4 GHz.

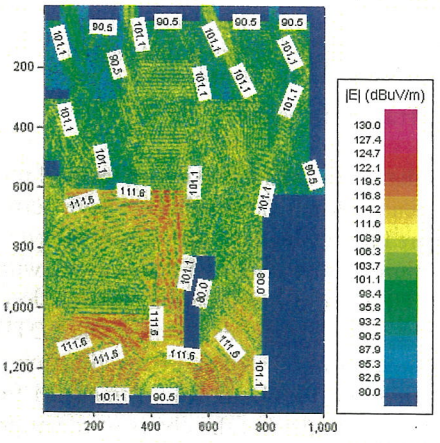

Fig. 9 Ray-tracing data 1.0 m above the floor at 5.2 GHz.

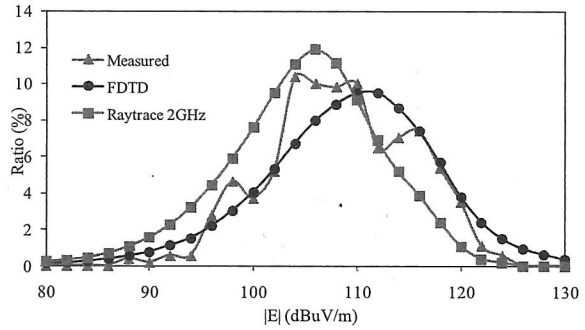

Fig. 10 Comparing 2.4 GHz FDTD, measurement & ray-tracing data.

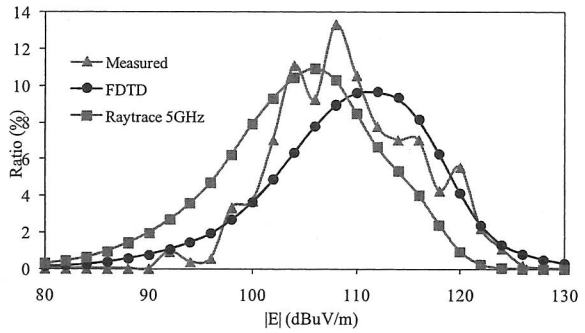

Fig. 11 Comparing 5.2 GHz FDTD, measurement & ray-tracing data.

There are a few areas between 104–116 dBμV/m where there is a difference between the FDTD and the measured values. However, upon detailed analysis of the calculated data, it has been observed that there are several instances where adjacent points (1 cm apart) are sometimes different in value by 3–7 dB. Therefore, it is possible that in the measurement process, a drift of just 1 or 2 cm away from the desired measurement point could result in values that skew the graph. Hence, the minor differences in Figs. 10 and 11 are thought to be due to measurement errors that would be very difficult to correct, given the complexity of the actual environment. It is therefore confirmed that the FDTD method is a valid technique for this type of environment since there is good agreement with established techniques. The applicability of the FDTD method in cases when humans are present will be examined in the next section.

4. Estimation of Human Absorption Effect

A refraction (bending) effect occurs on EM waves passing between mediums with different densities. This is also caused by a radio-frequency (RF) signal entering the human body since the body also absorbs the signal.

In this section, the human absorption effect for 802.11a is examined since it is expected to be noticeable. Homogenous phantom models are used. However, in-homogenous phantom model could also have been used but we consider the homogenous phantom to be suitable for obtaining precise field distributions in scenarios that requiring the estimation of absorption effects due to human bodies because

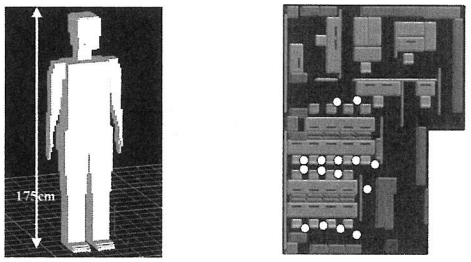

(a) Numerical Human Phantom Model (b) Positions of 15 humans

Fig. 12 Human phantom model used in simulation and example of randomly positioned humans throughout the room.

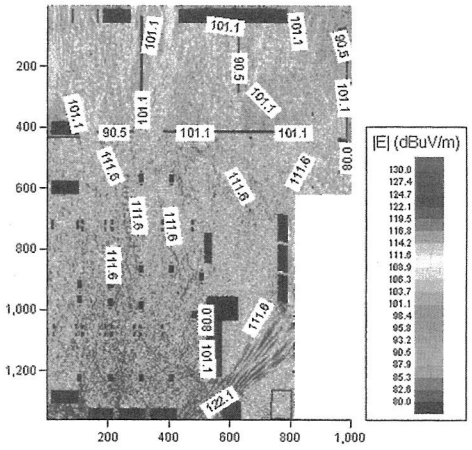

Fig. 13 FDTD data 1.0 m above the floor at 5.2 GHz with 15 persons.

most of the RF energy is absorbed on near-surface areas of the body.

These homogenous human phantom models are each 1.75 m tall and have a realistic shape as shown in Fig. 12(a). The electrical parameters are determined from 2/3 muscle equivalent tissue values that are two-thirds of the averaged value of muscle tissue for each frequency [15]. For 802.11a (5.2 GHz), the electrical parameters were: εr = 48.99, tan δ = 5.20. All of the other conditions of the previously simulated model remain the same with the only difference being that 15, 50 and 100 standing human phantom models are included. Figure 12(b) shows the phantoms' positions when 15 human models are scattered throughout the room.

Figure 13 illustrates electric field distribution in 2-D form in the plane 1 m above the floor for FDTD data with the same 15 persons that were present in Fig. 12(b). When this data is compared with the corresponding data for 5 GHz in Fig. 5, it is possible to see a reduction in the intensity of the distribution pattern in the region of the image that includes the humans. Figure 14 shows a histogram of the FDTD results for |E| as the number of human phantoms increases from 0 to 100. It is observed that there is a difference of 6 dB between the case with "0 humans" and the case with "100 humans."

In order to better visualize the field distribution char-

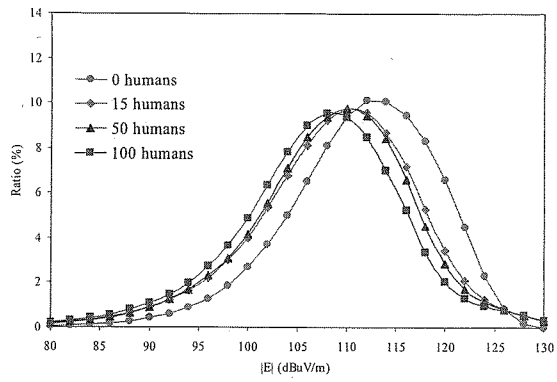

Fig. 14 5.2 GHz FDTD data with different numbers of humans present.

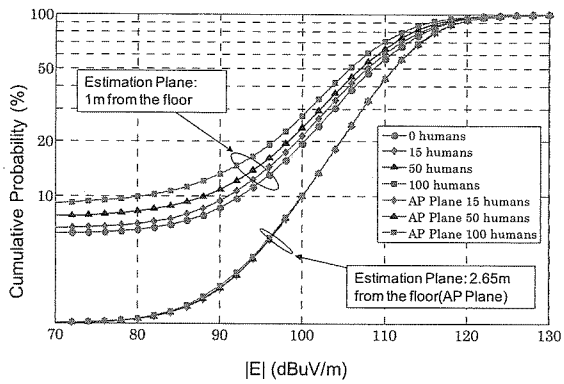

Fig. 15 Cumulative probability of 5.2 GHz FDTD data for different number of humans.

acteristics, the FDTD data (1.0 m from the floor) that was presented in Fig. 14 has also been included as a cumulative probability graph in Fig. 15. The figure also shows near Line-of-Sight propagation characteristics in the estimation plane of the AP in cases where 15, 50 and 100 persons were present in the room. The difference that is observed between these graphs at the AP height is negligible as the number of humans increases. This is the expected result since the height of the added humans is less than the height of the AP estimation plane. In this form, it can be deduced that the variation in |E| with the number of humans is greater in the plane 1 m from the floor as opposed to the AP plane.

Using the FDTD technique, it has been clearly shown that when human beings are present in a WLAN environment, received signal strength is affected because of the absorption of radiation energy by the human body.

5. Conclusions and Further Work

There is good correlation between measured data, Ray-tracing data and FDTD-obtained data. It should be noted that using in order to obtain the same level of precision in experimental data as is achieved in the FDTD calculations, over 1.3 million physical measurements need to be taken at points 1 cm from each other in the plane 1 m above the floor. For such a large and complex WLAN environment, this level of accuracy in measurements is not practical and therefore the FDTD method is a better method for cases such as these.

There will be further examination of the shape of the histograms in cases where the AP is moved to different positions throughout the room. In addition, if the number of APs in the environment is increased, it should be possible to see the impact on overall signal coverage, making it possible to determine the best overall design of the WLAN with respect to the location and number of APs.

The number of humans and the signal frequencies will also be varied to evaluate other realistic scenarios.

There will also be further investigations into the applicability of the ray-trace in cases where human phantom models are present. However, this paper has clearly established the applicability of large-scale FDTD analysis for indoor WLAN environments.

Acknowledgements

The authors wish to thank the High Performance Computing System at the Hokkaido University's Information Initiative Center for the use of its resources for the purpose of performing calculations.

References

[1] A. Hills, "Large-scale wireless LAN design," IEEE Commun. Mag., vol.39, no.11, pp.98–107, Nov. 2001.
[2] H. Nagatomo, Y. Yamada, K. Tabira, T. Itagaki, and S. Yuminaga, "Radiation from multiple reflected waves emitted by a cabin antenna in a car," IEICE Trans. Fundamentals, vol.E85-A, no.7, pp.1585–1593, July 2002.
[3] S. Horiuchi, K. Yamada, S. Tanaka, Y. Yamada, and N. Michishita, "Comparisons of simulated and measured electric field distributions in a cabin of a simplified scale car model," IEICE Trans. Commun., vol.E90-B, no.9, pp.2408–2415, Sept. 2007.
[4] T. Imai and T. Fujii, "Indoor micro cell area prediction system using ray-tracing method for mobile communication systems," Proc. IEEE Symp. Pers. Indoor Mob. Radio Commun. (PIMRC'96), pp.24–28, Oct. 1996.
[5] C.-F. Yang, B.-C. Wu, and C.-J. Ko, "A ray-tracing method for modeling indoor wave propagation and penetration," IEEE Trans. Antennas Propag., vol 46, no.6, pp.907–919, June 1998.
[6] Z. Zhang, R.K. Sorensen, Z. Yun, M.F. Iskander, and J.F. Harvey, "A ray-tracing approach for indoor/outdoor propagation through window structures," IEEE Trans. Antennas Propag., vol.50, no.5, pp.742–748, May 2002.
[7] Y. Wang, S. Safavi-Naeini, and S.K. Chaudhuri, "A hybrid technique based on combining ray tracing and FDTD methods for site-specific modeling of indoor radio wave propagation," IEEE Trans. Antennas Propag., vol.48, no.5, pp.743–754, May 2000.
[8] Y. Wang, S.K. Chaudhuri, and S. Safavi-Naeini, "An FDTD/ray-tracing analysis method for wave penetration through inhomogeneous walls," IEEE Trans. Antennas Propag., vol.50, no.11, pp.1598–1604, Nov. 2002.
[9] D.J. Cichon and J. Lahteenmake, "Ray optical propagation simulations & measurements in indoor environments," European Cooperation in the Field of Scientific & Technical Research EURO-COST 231 TD (94) 138, Darmstadt, Germany 1994.
[10] S.D. Gedney, "The application of the finite-difference time-domain method to EMC analysis," IEEE 1996 International Symposium on Electromagnetic Compatibility, Symposium Record, pp.117–121, Aug. 1996.

[11] A. Taflove, Computational Electromagnetics, Artech House, Boston, 1995.
[12] T. Taga and T. Imai, "Correlation characteristics between vertically and horizontally polarized components of arriving radio wave during shadowing by human body," Proc. International Symposium of Antennas and Propagation 2008, Oct. 2008.
[13] R.C. Dorf, The Electrical Engineering Handbook, CRC Press, 1993.
[14] K. Kunz and R. Luebbers, The Finite Difference Time Domain Method for Electromagnetics, CRC Press, 1993.
[15] C. Gabriel, "Compilation of the dielectric properties of body tissues at RF and microwave frequencies," Brooks Air Force Technical Report AL/OE-TR-1996-0037, 1996.

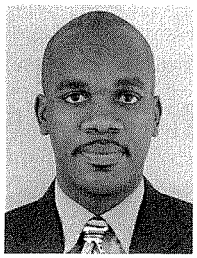

Louis-Ray Harris was born in Kingston, Jamaica in 1976. He received the B.Sc. in Electrical Engineering from the University of the West Indies, Trinidad, in 1999 and the M.Sc. in Space Communications Engineering from Lancaster University, England in 2001. He is currently studying for his Ph.D. in Wireless Communications Engineering at Hokkaido University, Japan. His current research areas are EMC and FDTD modelling.

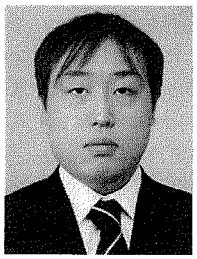

Takashi Hikage received the B.E., M.E. and Ph.D. degrees in electronics and information engineering from Hokkaido University, Sapporo, Japan, in 1997, 1999 and 2002, respectively. From 1999 to 2003, he was with the Graduate School of Engineering, Hokkaido University. Now, he is an Instructor of the Graduate School of Information Science and Technology, Hokkaido University, Sapporo. His research interests are FDTD analysis and EMC issues. Dr. Hikage is a member of the IEEE.

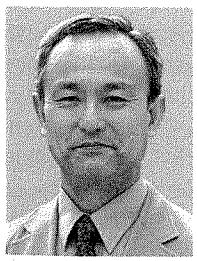

Toshio Nojima received a B.E. in electrical engineering from Saitama University, Japan in 1972 and received M.E. and Ph.D. degrees in electronic engineering from Hokkaido University in 1974 and 1988. From 1974 to 1992 he was with Nippon Telegraph and Telephone (NTT) Communications Laboratories, where he was engaged in the development of high-capacity microwave radio relay systems. From 1992 to 2001 he was with the Research Laboratory of NTT DoCoMo in Yokosuka, where he was a Senior Executive Research Engineer and conducted research on radio safety and EMC issues related to mobile radio systems as well as microwave circuit technologies. Since January of 2002 he has been a professor at the Graduate School of Information Science and Technology, Hokkaido University, Sapporo. Dr. Nojima is a member of the IEEE, the Institute of Electrical Engineers of Japan, and the Bioelectromagnetics Society.